

Structures and Molecular Surface Electrostatic Potentials of High-Density C, N, H Systems

Jane S. Murray,¹ Richard Gilardi,² M. Edward Grice,¹ Pat Lane,¹ and Peter Politzer^{1,3}

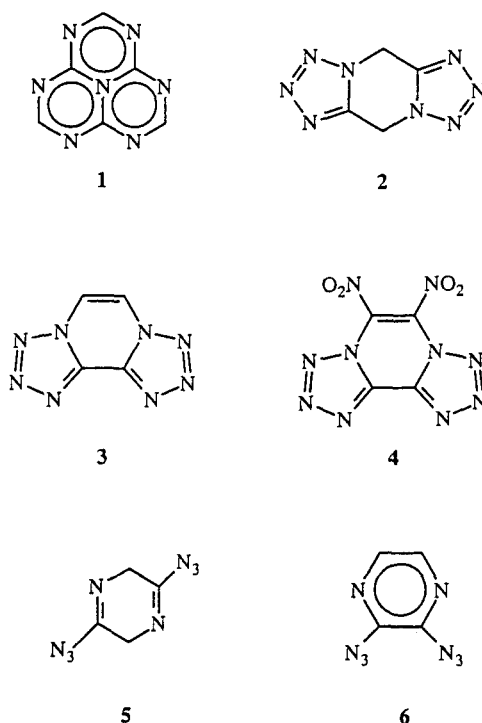
Received September 20, 1995; revised January 4, 1996, accepted January 15, 1996

Tri-*s*-triazine and two ditetrazolodiazines are known to have unusually high crystal densities (for unsubstituted C, N, H compounds). We have used a nonlocal density functional procedure to compute the geometries and energies of these and three related molecules, and then calculated the ab initio SCF electrostatic potentials on their molecular surfaces. We attribute the high densities to the relatively small molecular volumes and the strong intermolecular attractions arising from highly varying surface potentials. The energy differences of the two ditetrazoles and their diazide tautomers were computed, as well as for the dinitro derivative of one of the former.

KEY WORDS: High-density compounds; tri-*s*-triazine; ditetrazolodiazines; diazides; high-nitrogen compounds; surface electrostatic potentials.

INTRODUCTION

Since the detonation performance of an energetic material is directly related to its density [1], the latter property is an important criterion in evaluating prospective energetic compounds. To the best of our knowledge, the crystalline forms of **1–3** have the highest densities that have been measured for any unsubstituted C, N, H compounds: **1**, 1.69 g/cm³ [2]; **2**, 1.715 g/cm³ [3]; **3**, 1.674 g/cm³ [4]. It is accordingly interesting to consider these as possible starting points for energetic molecules such as **4**, the dinitro derivative of **3**. In this context, a potential concern in the cases of **2** and **3** would be any tendency to rearrange to the azides **5** and **6** [5–12]. This point shall be addressed. However, **1–3** do exist and form stable crystalline materials. It should be useful to investigate some of the properties of these molecules and simultaneously to try to gain some insight into the reasons for their high crystal densities. With



¹Department of Chemistry, University of New Orleans, New Orleans, Louisiana.

²Laboratory for the Structure of Matter, Naval Research Laboratory, Washington, DC.

³Correspondence should be directed to Peter Politzer, Department of Chemistry, University of New Orleans, New Orleans, Louisiana 70148.

these objectives, we have computed and analyzed their molecular electrostatic potentials, as well as those of **4–6**.

METHODS AND PROCEDURE

The electrostatic potential $V(\mathbf{r})$ created at any point \mathbf{r} by the nuclei and electrons of a molecule is defined rigorously by

$$V(\mathbf{r}) = \sum_A \frac{Z_A}{|\mathbf{R}_A - \mathbf{r}|} - \int \frac{\rho(\mathbf{r}') d\mathbf{r}'}{|\mathbf{r}' - \mathbf{r}|} \quad (1)$$

Z_A is the charge on nucleus A , located at \mathbf{R}_A , and $\rho(\mathbf{r})$ is the electronic density, which we obtain from the molecular wave function. $V(\mathbf{r})$ is a real physical property, which can be determined experimentally, by diffraction methods, as well as computationally [13]. It has proven to be a useful tool for predicting and interpreting molecular interactive behavior [13–15]. Regions of positive and negative potential on the molecular surface, defined as the 0.001 electron/bohr³ contour of $\rho(\mathbf{r})$ [16], are indicative of sites attractive to nucleophiles and electrophiles, respectively.

In recent years, we have developed more quantitative methods for using the electrostatic potential to analyze noncovalent molecular interactions [17–21]. We have introduced several statistically based indices that are defined in terms of the surface potential, two of which are

$$\Pi = \frac{1}{n} \sum_{i=1}^n |V(\mathbf{r}_i) - \bar{V}_S| \quad (2)$$

$$\sigma_{\text{tot}}^2 = \sigma_+^2 + \sigma_-^2 = \frac{1}{m} \sum_{i=1}^m [V^+(\mathbf{r}_i) - \bar{V}_S^+]^2 + \frac{1}{n} \sum_{j=1}^n [V^-(\mathbf{r}_j) - \bar{V}_S^-]^2 \quad (3)$$

In these equations, $V(\mathbf{r}_i)$ is the value of $V(\mathbf{r})$ at point \mathbf{r}_i on the surface, and \bar{V}_S is the average value of the potential on the surface. In a similar fashion, $V^+(\mathbf{r}_i)$ and $V^-(\mathbf{r}_j)$ are the positive and negative values of $V(\mathbf{r})$ on the surface, and \bar{V}_S^+ and \bar{V}_S^- are their averages:

$$\bar{V}_S^+ = \frac{1}{m} \sum_{i=1}^m V^+(\mathbf{r}_i) \quad \text{and} \quad \bar{V}_S^- = \frac{1}{n} \sum_{j=1}^n V^-(\mathbf{r}_j)$$

The index Π , given by Eq. (2), is the average deviation of the electrostatic potential on the molecular surface. We have shown that Π is an effective measure of local polarity (or charge separation), which may be quite significant even in a molecule having zero dipole moment, e.g. CO₂ and *p*-dinitrobenzene [17]. The total variance, σ_{tot}^2 , given by Eq. (3), is a measure of the spread of the values of the surface potential and is particularly sensitive to positive and negative extrema [18, 21].

In this work, molecular geometries and energies were computed with a nonlocal density functional procedure (GAUSSIAN 92/DFT [22], Becke exchange and Lee, Yang, and Parr correlation functionals [23, 24], 6-31G** basis set). Using these structures, the electrostatic potentials and related quantities were calculated at the ab initio HF/STO-5G level, in order that they be compatible with such data obtained earlier for other molecules [17–21, 25]. We have shown that the resulting trends in the surface electrostatic potentials are the same when the HF/6-31G* basis set is used [26].

RESULTS

Energies and structural data are shown in Table I. There is overall satisfactory agreement between the calculated (gas phase) and experimentally determined (crystalline) bond lengths for 1–3. An interesting feature of 1 is the near constancy of the bond lengths around its perimeter, contrasted to the considerably longer internal C–N bonds.

The surface electrostatic potentials of 1–6 are shown in Figs. 1–5. Their dominant features are the extensive positive regions above the heterocyclic rings. (Note, in Table II, the values of $V_{S,\text{max}}$, the most positive surface potentials.) Formally, all of these molecules are unsaturated and thus are expected to have pi electrons above the rings; in the case of benzene, for example, these produce a negative potential of –10.5 kcal/mole above the ring [27]. However, analogous negative regions are not found in 1–6, because of the effect of the strongly electron-attracting ring nitrogens; this has already been observed earlier for azines (e.g., 7–10) [27,



7



8



9



10

28]. The electron-withdrawing NO₂ groups in 4 cause the ring system to become even more positive (Fig. 3b and Table II).

The ring nitrogens on the peripheries of 1–6 have negative potentials of varying strengths associated with

Table I. DF/B-LYP/6-31G** Calculated Bond Distances and Energies and Experimentally Determined Bond Distances^a

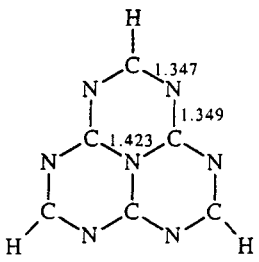
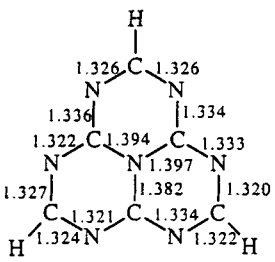
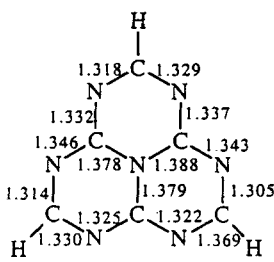
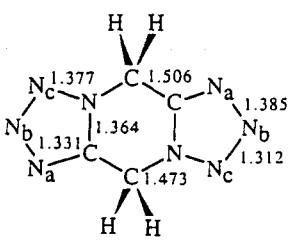
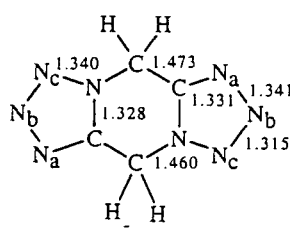
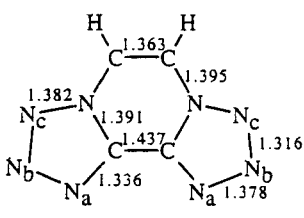
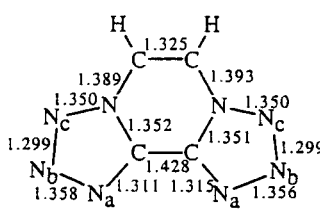
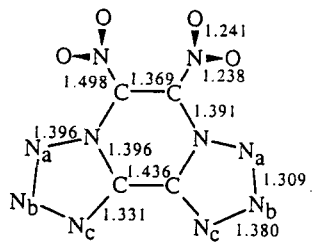
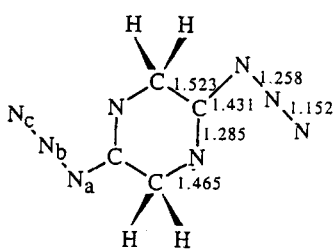
	Calculated bond distances (Å) and energy (hartrees)	Experimentally determined bond distances ^a (Å)
1	 <p>$E = -613.55104$</p>	 
2	 <p>$E = -592.60096$</p>	
3	 <p>$E = -591.39670$</p>	
4	 <p>$E = -1000.32701$</p>	-----
5	 <p>$E = -592.58066$</p>	-----

Table I. Continued.

Calculated bond distances (Å) and energy (hartrees)	Experimentally determined bond distances" (Å)
<p>6</p> <p>$E = -591.40491$</p>	-----

"The experimental data for 1, 2, and 3 are from Refs. 2-4, respectively.

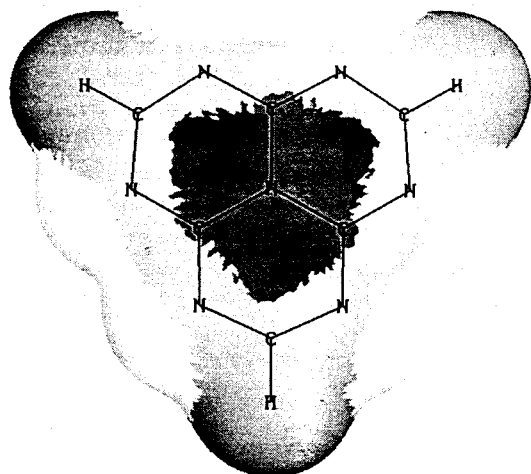


Fig. 1. Calculated electrostatic potential on the molecular surface of 1. Monochrome ranges, in kcal/mole, are: dark gray for $V(r) > 35$; light gray for $V(r)$ from 35 to 0; white for negative values of $V(r)$.

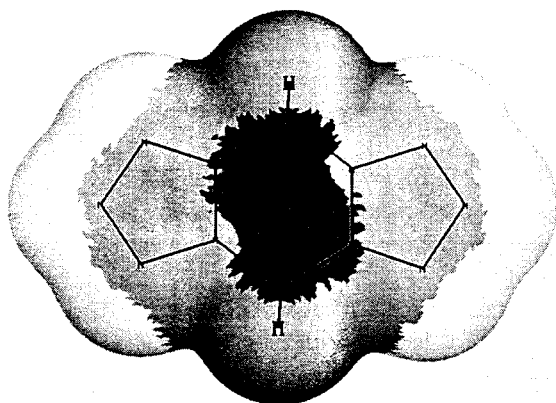
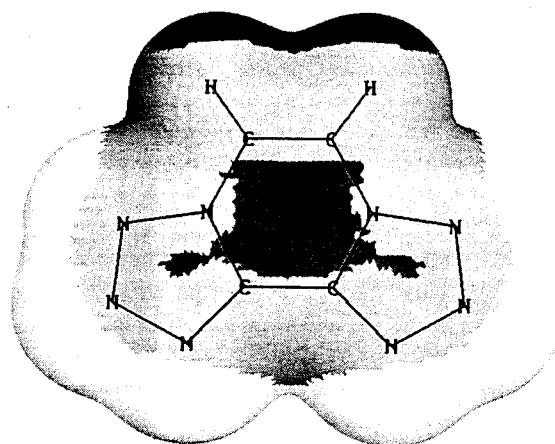
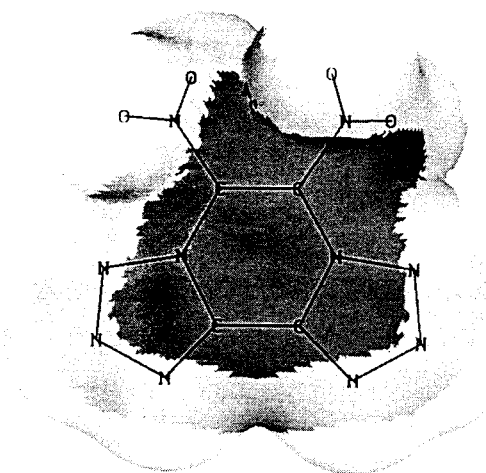


Fig. 2. Calculated electrostatic potential on the molecular surface of 2. Monochrome ranges, in kcal/mole, are: dark gray for $V(r) > 35$; light gray for $V(r)$ from 35 to 0; white for negative values of $V(r)$.



(a)



(b)

Fig. 3. Calculated electrostatic potential on the molecular surface of: (a) 3 and (b) its dinitro derivative 4. Monochrome ranges, in kcal/mole, are: dark gray for $V(r) > 35$; light gray for $V(r)$ from 35 to 0; white for negative values of $V(r)$.

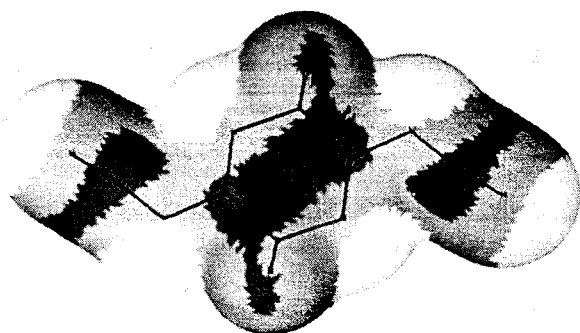


Fig. 4. Calculated electrostatic potential on the molecular surface of 5. Monochrome ranges, in kcal/mole, are: dark gray for $V(r) > 15$; light gray for $V(r)$ from 15 to 0; white for negative values of $V(r)$.

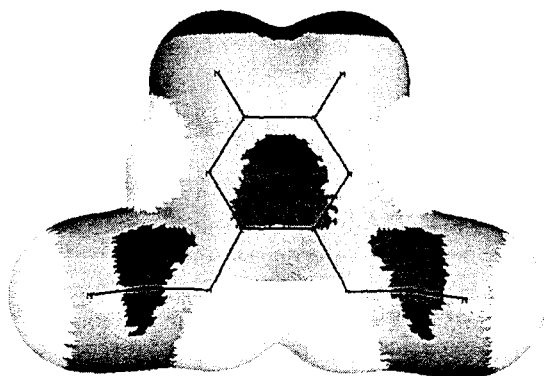


Fig. 5. Calculated electrostatic potential on the molecular surface of 6. Monochrome ranges, in kcal/mole, are: dark gray for $V(r) > 15$; light gray for $V(r)$ from 15 to 0; white for negative values of $V(r)$.

Table III. Most Negative Electrostatic Potentials, $V_{S,\min}(N)$ and $V_{\min}(N)$, Associated with the Nitrogens in the Azides 5 and 6^a

Molecule	$V_{S,\min}(N)$, kcal/mole	$V_{\min}(N)$, kcal/mole
5	N_{ring} : -32.6	N_{ring} : -72.2
	N_a : -29.3	N_a : -57.9
	N_b : none found	N_b : none found
	N_c : -19.7	N_c : -28.0
6	N_{ring} : -28.6	N_{ring} : -65.9
	N_a : -49.2 ^b	N_a : -68.3
	N_b : none found	N_b : none found
	N_c : -19.9	N_c : -28.1

^aThe labeling of the nitrogens follows Table I.

^bThe negative surface region associated with each N_a overlaps that of the other, and there is only one local minimum.

their lone pairs. Tables II and III list their most negative values on the molecular surfaces, $V_{S,\min}(N)$, and also in three dimensions, $V_{\min}(N)$. The triply coordinated nitrogens in the central portions of the molecules have no negative potentials at all. The peripheral nitrogens accordingly have some basic character and some hydrogen-bond-accepting tendencies, although relatively weak; among the known compounds 1-3, the strongest in both respects should be 1, for which the present results combined with our earlier correlations [29, 30] suggest a pK_a of about 0.0 and a hydrogen-bonding ability similar to that of pyrazine, 7. It might have been anticipated that 1 will be similar to *s*-triazine (8) in these properties, but the negative potentials in 1 are actually stronger than in 8; e.g., $V_{\min}(N)$ is -80.0 kcal/mole in the former and -74.6 kcal/mole in the latter [28]. This

Table II. Calculated and Experimental Properties of 1-4^a

Molecule	Density	Surface		$V_{S,\max}$	$V_{S,\min}(N)$	$V_{\min}(N)$	II	σ_+^2	σ_-^2	σ_{tot}^2
		area	Volume ^b							
1	1.689 ^c	163.9	145.4	52.2	-43.2	-78.1	21.2	181.7	172.3	354.0
2	1.715 ^d	162.0	141.7	53.7	N_a : -38.9	N_a : -72.0	23.4	111.9	126.3	283.2
					N_b : -42.8	N_b : -70.9				
					N_c : -28.5	N_c : -52.3				
3	1.674 ^e	153.3	133.7	50.2	N_a : -25.4	N_a : -47.7	24.7	130.6	137.0	267.6
					N_b : -41.4	N_b : -68.8				
					N_c : -44.0	N_c : -73.3				
4	—	200.0	174.3	72.0	N_a : -18.6	N_a : -48.6	21.6	358.6	64.3	422.9
					N_b : -31.3	N_b : -54.9				
					N_c : -32.2	N_c : -57.9				

^aUnits: density, g/cm³; area, Å²; volume, Å³; all potentials and II, kcal/mole; σ_+^2 , σ_-^2 , and σ_{tot}^2 (kcal/mole)².

The labeling of the nitrogens follows Table I.

^bReference 36.

^cReference 2.

^dReference 3.

^eReference 4.

is presumably because the peripheral nitrogens in **1** withdraw some electronic charge from the one in the center of the molecule, which is formally positive. The least basic ring nitrogens, overall, are those in **4**, which have lost a portion of their electronic charge to the nitro groups.

Table II also contains the calculated areas and volumes of **1–4**, based on the 0.001 au contour of the electronic density, as well as several properties computed from the surface electrostatic potentials: Π , σ_+^2 , σ_-^2 , and σ_{tot}^2 . The Π values of **1–4** show that these molecules have high degrees of internal charge separation, as can also be seen in Figs. 1–3. For **1–4**, Π ranges from 21 to 25 kcal/mole, although we have usually found it to be between 2 and 15 kcal/mole for organic molecules [17]. Structures **1–4** are good examples of how local polarity, as measured by Π , may differ from net overall polarity, given by the dipole moment. Structures **1** and **2** have high values of Π , even though their dipole moments are zero, due to symmetry. Both **3** and **4** have nonzero dipole moments, but that of **3** is much larger, 6.12 compared to 1.24 Debyes, at the HF/STO-5G//HF/3-21G level; this is because the polarity of the NO₂ groups in **4** is opposite in direction to that of the ring nitrogens. However the Π values of **3** and **4** are nearly the same (Table II).

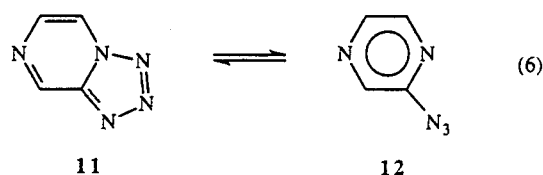
The magnitudes of σ_{tot}^2 are also large, between 238 and 354 (kcal/mole)² for **1–3**, and 423 (kcal/mole)² for **4**, whereas we usually find it to be below 180 (kcal/mole)² [18, 19]. The high values of σ_{tot}^2 for **1–4** suggest strong electrostatic interaction tendencies. Although Figs. 1–3a show that the molecular surfaces of **1–3** are largely positive, the approximate similarity of σ_+^2 and σ_-^2 in each case indicates that the variation in the positive and negative potentials is roughly the same. In marked contrast, the positive potentials in **4** are clearly much greater in magnitude than are the negative, as well as more extensive; this is seen in Fig. 3b and in the fact that $\sigma_+^2 \gg \sigma_-^2$.

DISCUSSION

The possibility of tetrazolo-azido tautomerism is well established for nitrogen heterocyclic systems [5–12]; for **2** and **3** it is represented by



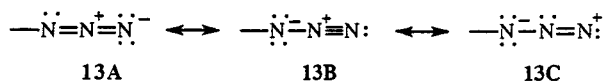
The general experience has been that the tetrazolo tautomers appear to be favored by a high electronic density associated with the central heterocyclic ring and in particular with the nitrogen that is common to both rings in the tetrazolo form [5–9]; thus, electron-withdrawing substituents tend to promote the azido tautomer. However, environmental factors can be extremely important [5–12]; for example, the equilibrium shown in Eq. (6) has been observed in chloroform and in trifluoroacetic acid solutions [6], but only **11** is present in the solid phase [31].



From our computed energies in Table I, we obtain $\Delta E = 12.7$ kcal/mole for Eq. (4) and $\Delta E = -5.2$ kcal/mole for Eq. (5). Since we find **6** to be slightly more stable than **3** on a molecular level, the fact that **3** is the form that is observed in the solid phase [4] is presumably due to stabilization provided by crystal lattice interactions.

In seeking to understand the contrast between the equilibria in Eqs. (4) and (5), wherein the former favors the tetrazole and the latter the azide, it is useful to look at the computed electrostatic potentials of the two azides, **5** and **6**; these are shown, on the molecular surfaces, in Figs. 4 and 5. The minima associated with the nitrogens, both $V_{S,\text{min}}(\text{N})$ and $V_{\text{min}}(\text{N})$, are listed in Table III.

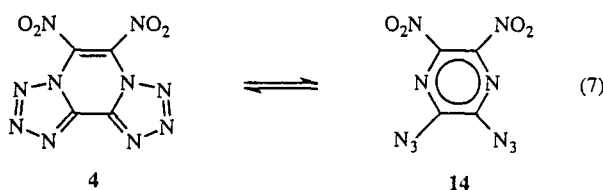
An interesting feature of these results is the charge distribution in the azido group. Table III and Figs. 4 and 5 show that the central nitrogen is positive in character, while the linking one is strongly negative; the outermost nitrogen is intermediate between these extremes. Thus, in terms of the resonance description of the azido group given in **13A–13C**, the dominant contributors appear to be **13A** and **13B**. This conclusion is consistent with the



structural data in Table I, as well as with earlier interpretations [32].

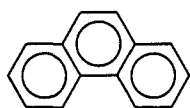
Table III also reveals the ring nitrogens in **5** to be more negative than in **6**. In this respect, therefore, our finding that the tetrazole is more favored energetically in Eq. (4) than in Eq. (5) is in agreement with the past experience mentioned earlier [5–9].

However, this introduces a serious question concerning **4**, the dinitro derivative of **3**. We did verify that the optimized geometry of **4** corresponds to a true energy minimum; there are no imaginary vibrational frequencies [33]. On the other hand, since the azido tautomer **6** is already slightly more stable than the tetrazole **3**, and electron-withdrawing groups such as NO₂ promote the formation of the azide, it may be that the azido tautomer **14** is considerably favored energetically over **4**:

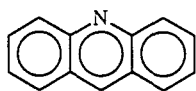


We have accordingly computed an optimized geometry and energy for **14**, using the Gaussian 92/DFT procedure described earlier [22–24]. The resulting energy, -1000.37066 hartrees, yields $\Delta E = -27.4$ kcal/mole for Eq. (7). This confirms that the introduction of nitro groups in **3** will be expected to shift the tautomeric equilibrium significantly toward the azide. This is unfortunate from the standpoint of an energetic material, because of the well-known proclivity of many azides for facile decomposition [32].

The density of a molecular crystal depends upon the mass and size of the molecule and upon the crystal-line structure and packing. It is interesting to compare **1–3** to phenanthrene (**15**) and acridine (**16**). The molecular weights of the first three are somewhat less than those of the last two, yet the densities of **1–3** are more than 30% greater than those of **15** and **16** [34]. Much



15



16

of this difference can be attributed to the smaller volumes of **1–3** (Table II), all of which are at least 25% less than the 201.4 Å³ of **15** and 199.3 Å³ of **16** [35].

This is fully consistent with the findings of Stine, who analyzed the crystal structures of more than 2000 organic compounds to obtain effective volumes for their

constituent atoms in various bonding environments [36]. He concluded that, in general, high densities are promoted by maximizing the numbers of nitrogens and oxygens and minimizing the numbers of carbons and hydrogens.

Molecular interactions are also expected to play a role in determining the densities of organic compounds. We have found σ_{tot}^2 to be an effective measure of this for crystal densities [25] as well as for a variety of other macroscopic properties, including critical constants, boiling points, heats of vaporization, partition coefficients, and supercritical solubilities [18–21, 25]. Since density increases with σ_{tot}^2 [25], the large magnitudes of the latter property for **1–3**, greatly exceeding the σ_{tot}^2 values of typical organic compounds (as pointed out above), are a second factor in the high densities of **1–3**, in addition to their relatively small sizes.

SUMMARY

We suggest that the high densities found crystallographically for **1–3** can be attributed to their relatively small molecular volumes and the strong intermolecular attractions arising from the highly varying electrostatic potentials on their molecular surfaces. Structures **3** and **4** can be involved in tautomeric equilibria with diazides, and in the gas phase, **3** is 5.2 kcal/mole more stable as the diazide, although in the crystal it exists only as the tetrazole. In the dinitro derivative of **3**, the energetic preference for the diazide tautomer is greatly enhanced, indicating that its usefulness as an energetic material is open to question.

ACKNOWLEDGMENT

We appreciate the financial support of the office of Naval Research through contract no. N00014-95-1-0028 and program officer Dr. Richard S. Miller.

REFERENCES

1. Kamlet, M. J.; Jacobs, S. J. *J. Chem. Phys.* **1968**, *48*, 23.
2. Hosmane, R. S.; Rossman, M. A.; Leonard, N. J. *J. Am. Chem. Soc.* **1982**, *104*, 5497.
3. Gilardi, R.; George, C.; Flippen-Anderson, J. L. Naval Research Laboratory, Annual Report to Office of Naval Research; Arlington, VA 22217, 1986.
4. Gilardi, R.; George, C.; Flippen-Anderson, J. L. Naval Research Laboratory, Annual Report to Office of Naval Research; Arlington, VA 22217, 1985.

5. Boyer, J. H.; Miller, E. J., Jr. *J. Am. Chem. Soc.* **1959**, *81*, 4671.
6. Wentrup, C. *Tetrahedron* **1970**, *26*, 4969.
7. Sasaki, T.; Kanematsu, K.; Murata, M. *J. Org. Chem.* **1971**, *36*, 446.
8. Tisler, M. *Synthesis* **1973**, 123.
9. Goodman, M. M.; Atwood, J. L.; Carlin, R.; Hunter, W.; Paudler, W. W. *J. Org. Chem.* **1976**, *41*, 2860.
10. Neunhoeffer, H. In *Comprehensive Heterocyclic Chemistry*; Boulton, A. J.; McKillop, A. Eds.; Pergamon: Oxford, 1984; Vol. 3, Part 2B; ch. 2.19.
11. Denisov, A. Y.; Krivopalov, V. P.; Mamatyuk, V. I.; Mamaev, V. P. *Magn. Reson. Chem.* **1988**, *26*, 42.
12. Krivopalov, V. P.; Baram, S. G.; Denisov, A. Y.; Mamatyuk, V. I. *Izv. Akad. Nauk., SSSR, Ser. Khim.* **1989**, *9*, 2002.
13. Politzer, P.; Truhlar, D. G. *Chemical Applications of Atomic and Molecular Electrostatic Potentials*; Plenum Press: New York, 1981.
14. Scrocco, E.; Tomasi, J. *Adv. Quant. Chem.* **1978**, *11*, 115.
15. Politzer, P.; Murray, J. S. In *Reviews in Computational Chemistry*; Lipkowitz, K. B.; Boyd, D. B., Eds.; VCH: New York, 1991; Vol. 2; ch. 7.
16. Bader, R. F. W.; Carroll, M. T.; Cheeseman, J. R.; Chang, C. *J. Am. Chem. Soc.* **1987**, *109*, 7968.
17. Brinck, T.; Murray, J. S.; Politzer, P. *Mol. Phys.* **1992**, *76*, 609.
18. Politzer, P.; Murray, J. S.; Lane, P.; Brink, T. *J. Phys. Chem.* **1993**, *97*, 729.
19. Brinck, T.; Murray, J. S.; Politzer, P. *J. Org. Chem.* **1993**, *58*, 7070.
20. Murray, J. S.; Lane, P.; Brinck, T.; Paulsen, K.; Grice, M. E.; Politzer, P. *J. Phys. Chem.* **1993**, *97* 9369.
21. Murray, J. S.; Brinck, T.; Lane, P.; Paulsen, K.; Politzer, P. *J. Mol. Struct. (Theochem)* **1994**, *307*, 55.
22. Frisch, M. J.; Trucks, G. W.; Schlegel, H. B.; Gill, P. M. W.; Johnson, B. G.; Wong, M. W.; Foresman, J. B.; Robb, M. A.; Head-Gordon, M.; Replogle, E. S.; Gomperts, R.; Andres, J. L.; Raghavachari, K.; Binkley, J. S.; Gonzalez, C.; Martin, R. L.; Fox, D. J.; DeFrees, D. J.; Baker, J.; Stewart, J. J. P.; Pople, J. A. GAUSSIAN 92/DFT, Gaussian, Inc.: Pittsburgh, PA, 1993.
23. Becke, A. D. *Phys. Rev. A* **1988**, *38*, 3098.
24. Lee, C.; Yang, W.; Parr, P. G. *Phys. Rev. B* **1988**, *37*, 785.
25. Murray, J. S.; Brinck, T.; Politzer, P. *Chem. Phys.* **1996**, *204*, 289.
26. Murray, J. S.; Lane, P.; Politzer, P. *Mol. Phys.* **1995**, *85*, 1.
27. Politzer, P.; Murray, J. S.; Seminario, J. M.; Miller, R. S. *J. Mol. Struct. (Theochem)* **1992**, *262*, 155.
28. Murray, J. S.; Seminario, J. M.; Politzer, P. *J. Mol. Struct. (Theochem)* **1989**, *187*, 95.
29. Brinck, T.; Murray, J. S.; Politzer, P.; Carter, R. E. *J. Org. Chem.* **1991**, *56*, 2934.
30. Murray, J. S.; Politzer, P. *J. Chem. Res.* **1992**, *S*, 110.
31. Rutner, H.; Spoerri, P. E. *J. Heterocyclic Chem.* **1996**, *3*, 435.
32. Boyer, J. H.; Canter, F. C. *Chem. Rev.* **1954**, *54*, 1.
33. Hehre, W. J.; Radom, L.; Schleyer, P. v. R.; Pople, J. A. *Ab Initio Molecular Orbital Theory*; Wiley-Interscience: New York, 1986.
34. Dean, J. A. *Lange's Handbook of Chemistry*, 14th ed.; McGraw-Hill: New York, 1992.
35. DeSalvo, M.; Miller, E.; Murray, J. S.; Politzer, P., unpublished work.
36. Stine, J. R. In *Structure and Properties of Energetic Materials*; Liebenberg, D. H.; Armstrong, R. W.; Gilman, J. J., Eds.; Materials Research Society: Pittsburgh, 1993.